Chalcogenide Letters Vol. 21, No. 6, June 2024, p. 483 - 491

Structural, morphological, optical and low temperature magnetic studies on $SnSeO_3/ZnSeO_3$ nanocomposite

N. G. Basil Ralph[a], S. Shanmugha Soundare[b], R. Harshinee[a], S. Ariponnammal[a,*]
[a]*Department of Physics, Gandhigram Rural Institute, Deemed To Be University, Gandhigram-624302, Dindigul District, Tamilnadu, India*
[b]*Centre for Nanoscience and Technology, Anna University, Chennai-600025, Tamilnadu, India*

Nanocomposite $SnSeO_3/ZnSeO_3$ has been synthesized by hydrothermal method. EDAX and XRD confirm the perfect formation of $SnSeO_3/ZnSeO_3$ nano composite. It shows an interesting morphology of rectangular bar. Particle size is determined as 137.3nm. It is an effective applicant for applications in optoelectronic field. The energy gap of $SnSeO_3/ZnSeO_3$ nanocomposite is 5.52 eV. Urbach energy value obtained is 0.0635 eV. Refractive index obtained from optical energy gap is 1.926. PL emission spectrum obtains a strong efficient emission in UV (~387.7 nm) region, weak emission in green (~520.7 nm) region, and moderate emission in red (~788.7 nm) region. The UV emission at 387.7 nm shows radiative electron-hole recombination and it makes the candidate suitable for display applications. The emission peaks in the visible range may be attributed to different surface imperfections of Schottky and Frenkel kinds, oxygen vacancies and Sn – interstitials or Zn -interstitials. The FTIR bands are well assigned and confirms Se-O, Zn-O, Sn-O bonds in finger print region. The sample exhibits diamagnetic nature at 300K and 5K. It also exhibits interesting super paramagnetic nature at 5K between -0.15Tesla to 0.15Tesla.

(Received March 27, 2024; Accepted June 17, 2024)

Keywords: $SnSeO_3/ZnSeO_3$, Nanocomposite, Structural, Morphological, Optical, Low temperature magnetic studies

1. Introduction

Oxy chalcogenides, also known as chalcogen-based oxides, are a new class of materials that combine oxygen (O) with one or more elements from the chalcogen group, which includes sulfur (S), selenium (Se), and tellurium (Te). These compounds exhibit interesting physical and chemical properties due to the combination of oxygen's electronegativity and the unique characteristics of chalcogen elements. Oxy chalcogenides have attracted significant attention in materials science and solid state physics due to their diverse range of properties and potential applications. They exhibit a wide range of electrical, magnetic, optical, and catalytic behaviours, which make them useful in various technological applications [1]. Oxy chalcogenides can be synthesized using different methods, including solid-state reactions, hydrothermal synthesis, sol-gel processes, and chemical vapour deposition. The choice of synthesis method depends on the desired properties and the specific applications [2]. They can have a variety of crystal structures, including layered, perovskite-like, and tunnel structures. The arrangement of atoms within the crystal lattice affects the physical properties of the material, such as electrical conductivity, bandgap, and magnetic ordering[3]. They exhibit a wide range of electrical conductivity, ranging from insulating to semiconducting and even metallic behaviour. This variability in conductivity makes them suitable for applications in electronics, energy storage, and catalysis [4]. Some oxy chalcogenides exhibit interesting magnetic properties, such as ferromagnetic, antiferromagnetic, or spin-glass behaviour. These materials can be used in spintronics, magnetic storage devices, and sensor applications[5]. They can possess unique optical properties, including a wide range of bandgaps and strong light-matter interactions. These properties make them useful in

* Corresponding author: ariponnammal@gmail.com
https://doi.org/10.15251/CL.2024.216.483

optoelectronics, photocatalysis, and solar energy conversion applications [6]. They have shown promising catalytic activity for various chemical reactions, including, water splitting, pollutant degradation, and CO_2 reduction. Their catalytic performance arises from the synergistic effects between oxygen and chalcogen species, leading to enhanced reactivity and selectivity[7]. Some oxy chalcogenides have been investigated for energy storage applications, particularly in rechargeable batteries and supercapacitors. Their unique combination of electrical and chemical properties can improve energy storage performance and increase device efficiency[8]. Oxy chalcogenides have also been explored for environmental applications, such as water purification, air pollution control, and photocatalytic degradation of organic pollutants. Their ability to activate oxygen and generate reactive species makes them effective in environmental remediation processes [9]. Oxy chalcogenides continue to be an active area of research, with ongoing efforts to discover new compositions, understand their fundamental properties, and explore novel applications. Researchers are investigating their potential in areas like quantum computing, thermoelectric devices, and emerging nanoelectronics [10]. In summary, oxy chalcogenides represent a versatile class of materials with a wide range of properties and applications. Their combination of oxygen and chalcogen elements offers unique opportunities for tailoring their properties to meet specific technological needs, making them valuable in various fields of science and technology. This paper deals with study on oxy chalcogenide nanocomposite $SnSeO_3/ZnSeO_3$.

2. Methods and materials

The hydrothermal technique was utilized to produce the nanocomposite $SnSeO_3/ZnSeO_3$. Alfa Aesar analytical grade chemicals of 0.1M $ZnCl_3$, 0.1M $SnCl_3$, and 0.1M Na_2SeO_3 are dissolved in 30:30:30ml of double-distilled water. At regular intervals, freshly generated aqueous 0.1M Na_2TeO_3 solution was combined with 0.1M $ZnCl_3$, 0.1M $SnCl_3$ solution drop by drop with continuous stirring at a rate of 400 rpm. Then, the whole solution is transferred into teflon container in an autoclave and kept at a constant temperature of 60°C for about 8 hours. After cooling, a grey white precipitate was obtained. It is centrifuged after being cleaned numerous times, first with double distilled water and then with ethanol. The precipitate was subsequently dried at 50 °C for a few hours before being placed in desiccator for storage.

The Energy dispersive X-ray analysis spectrum (EDAX) is recorded by the OXFORD INCAPENTAx3 model in England. The Carel ZEISS EVO-18 model is utilized to record scanning electron microscopy (SEM) and X-ray powder diffraction (XRD) by Panalytical X'Pert Pro using Cu Kα radiation. The Perkin Elmer Lambda 35 spectrophotometer is used to obtain the ultraviolet-visible (UV-Vis) spectrum; the VARIAN Cary Eclipse Fluorescence Spectrophotometer is used to obtain the photoluminescence (PL) spectrum; the Perkin Elmer BX model spectrophotometer is used to obtain the Fourier transform infrared (FTIR) spectrum; and the Lakeshore model VSM 7410 is used for magnetic measurements.

3. Results and discussions

3.1. Morphological studies

Figure 1 shows EDAX of $SnSeO_3/ZnSeO_3$ nano composites sample. It is observed that the sample consists of Sn, Zn, Se and O elements, confirming the product purity. The observed weight percentages of Tin, Zinc, Selenium and Oxygen are 32.07%, 12.99%, 18.30% and 36.64% respectively. The analysis confirms the perfect formation of $SnSeO_3/ZnSeO_3$ nano composite. SEM picture of $SnSeO_3/ZnSeO_3$ at magnification of 25 KX (Figure 2) shows an appealing morphology of rectangular bar. Particle size is determined as 137.3nm using particle size analyser.

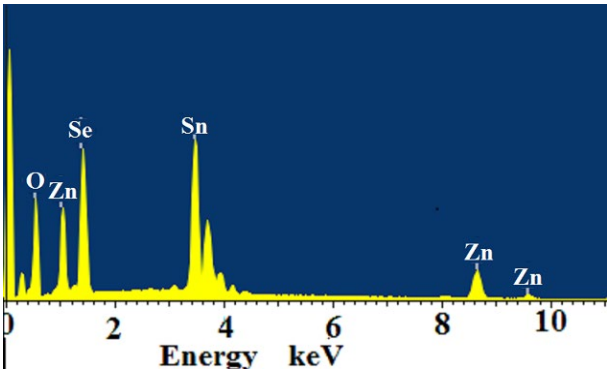

Fig. 1. EDAX of $SnSeO_3/ZnSeO_3$ nanocomposite.

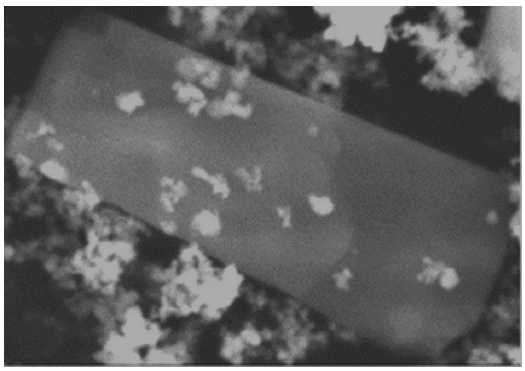

Fig. 2. SEM picture of $SnSeO_3/ZnSeO_3$ nanocomposite.

3.2. XRD

Figure 3 depicts XRD of $SnSeO_3/ZnSeO_3$ nano composites synthesized by simple hydrothermal method. The phase structure of products was characterized. It has been found out that the high intensity peaks are appeared at 2θ values for $SnSeO_3$ at 13.2604, 19.7609, 20.4787, 26.6774, 40.5178, 41.8944, 43.6434 and 51.7225, which are indexed with the planes of (100),(011), (101), (120), (122), (202), (212) and (023) with orthorhombic structure with lattice parameters of a = 6.350 Å, b = 8.224 Å, and c = 5.852 Å,[11] and $ZnSeO_3$ at 29.7772, 31.4029, 49.8843, 54.9864, 55.8340 and 65.0668 which are indexed with planes of (020), (021), (123), (301), (310) and (303) at orthorhombic structure with lattice parameters of a=5.14 Å, b = 6.00 Å, and c = 7.81 Å[12].

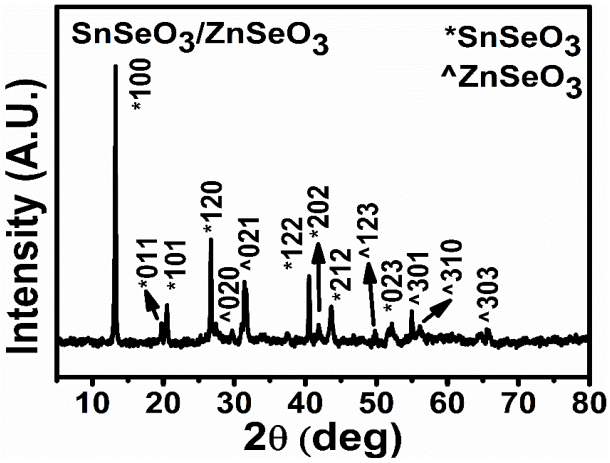

Fig. 3. XRD of $SnSeO_3/ZnSeO_3$ nanocomposite.

Further, absence of alloy peaks and no peak shifts confirmed the perfect formation of $SnSeO_3/ZnSeO_3$ [13].

3.3. Optical studies

Figure 4 displays recorded UV-VIS spectrum. It is appropriate for use as a filter in the UV zone due to its strong absorption at roughly 209.39 nm. UV light is divided into four regions as vacuum UV (10-200 nm), far UV (200-280 nm), near UV (280-400 nm), and visible UV (400-800 nm). The vacuum UV region has the highest energy and shortest wavelength, while the visible UV region has the lowest energy and longest wavelength. $SnSeO_3/ZnSeO_3$ nanocomposite only absorbs light in the vacuum UV region. It means that the energy gap between its ground state and its first excited state is very large, and only light with very high energy can excite the electrons in $SnSeO_3/ZnSeO_3$ nanocomposite sample[14].

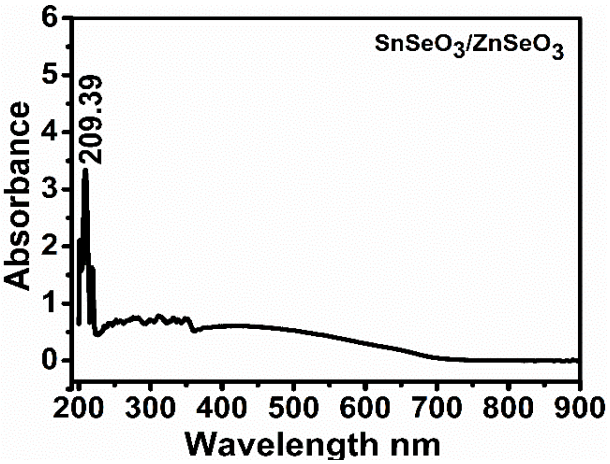

Fig. 4. UV –Visible absorbance spectrum of $SnSeO_3/ZnSeO_3$ nanocomposite.

Light with lower energy, such as short, middle, and long UV light, does not have enough energy to overcome the energy gap, and therefore passes through $SnSeO_3/ZnSeO_3$ without being absorbed. A small absorption in the visible region means that the sample has a low concentration of chromophores, or molecules that can absorb light in that range. Chromophores usually have conjugated double bonds or aromatic rings that can undergo electronic transitions when exposed to light. The light absorbed by a sample is in proportion to the chromophores concentration, according to the Beer-Lambert law [14-16]. Therefore, a small absorption implies a low concentration of chromophores, or a high transmittance of light through the sample. Alternatively,

a small absorption could also mean that the sample has a very short path length, or a low molar absorptivity of chromophores [14-16]. These factors also affect the absorbance of light by a sample, as shown by the equation

$$A = \in cl \tag{1}$$

Here, A is absorbance, $\in$ is molar absorptivity, c is concentration, and l is path length [14]. Thus, the transmittance is observed to be high in the visible region due to the lower concentration of chromophores. The broad transmission spanning from 250 to 900 nm makes the $SnSeO_3/ZnSeO_3$ nanocomposite a viable candidate for use in optoelectronic applications. A Taue plot of $(\alpha h\upsilon)^2$ against energy is depicted in Figure 5, and it indicates an energy gap of 5.52 eV for the $SnSeO_3/ZnSeO_3$ nanocomposite [17–18].

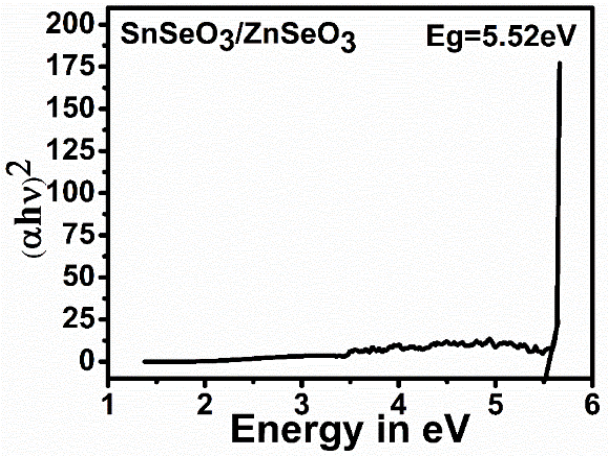

Fig. 5. Taue plot of $SnSeO_3/ZnSeO_3$ nanocomposite.

The Urbach energy value of 0.0635 eV is derived from the Urbach plot (Figure 6). Using relation (2) [19–20], the refractive index derived using the optical energy gap is 1.926.

$$\frac{n^2-1}{n^2+2}=1-\sqrt{\frac{E_{opt}}{20}} \tag{2}$$

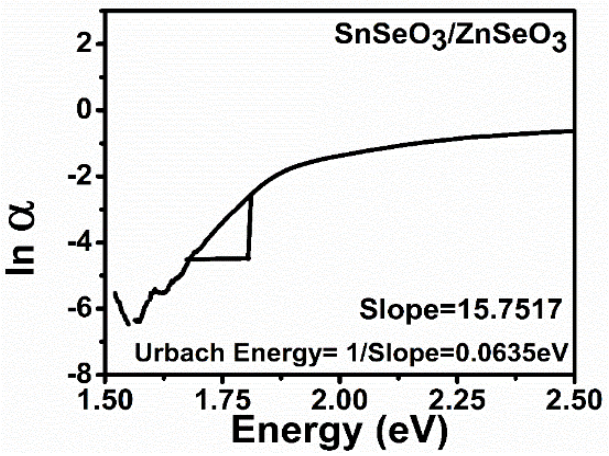

Fig. 6. Urbach plot of $SnSeO_3/ZnSeO_3$ nanocomposite.

Figure 7 depicts PL emission spectrum with excitation at 395 nm. It exhibits strong effectual emission in UV (~387.7 nm) region, weak green emission (~520.7 nm) region, and moderate red emission (~788.7 nm) region. The peak in the UV region at 387.7nm is the envelope of phonon replicas of free exciton luminescence as reported in ZnO [21]. It may be due to radiative electron-hole recombination. The deep UV region peak makes the candidate a promising material for display applications [22]. Different surface imperfections of the Schottky and Frenkel kinds can be blamed for the emission peak in the visible range.

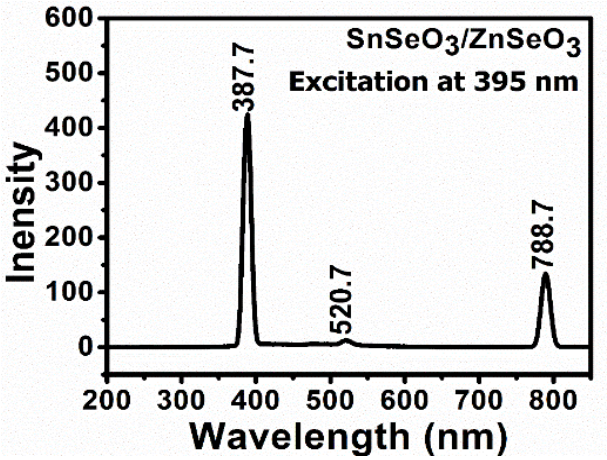

Fig. 7. PL spectrum of $SnSeO_3/ZnSeO_3$ nanocomposite.

Oxygen vacancies and interstitials are normally extremely common in oxide systems, and their appearance greatly influences the modified photoluminescence response [23-27]. Minor intensity peak at 520.7nm is ascribed to oxygen vacancies and Sn –interstitials or Zn -interstitials. The medium intensity peak at 788.7 nm corresponds to Sn-interstitial defects[28]. Nanoparticles have the potential to be employed as optoelectronic devices, luminescence detectors, and ultraviolet photo-conductive detectors [26].

3.4. FTIR study

Figure 8 shows FTIR spectrum of $SnSeO_3/ZnSeO_3$ nanocomposite. It shows broad trough from 3680.18 and 2376.30 cm^{-1} enclosing a peak centered at 3394.72 cm^{-1} is assigned as O-H bond [29-31]. Also, O-H bonds are ascribed to the bands seen at 1635.64, 1442.75, and 1381.03. These have provided clues regarding the hygroscopic quality of the material. The fingerprint region is made up of bands that correspond to the Se-O bond at 848.68 [32], the Zn-O bond at 763.81 and 470.63 cm-1 [33, 34], and the Sn-O bond at 686.66 and 563.21 cm^{-1} [35].

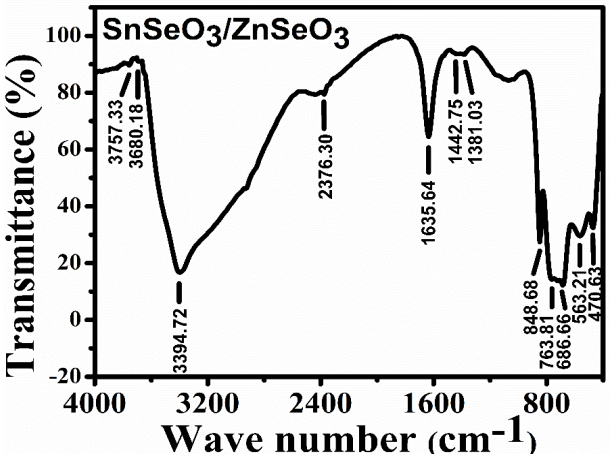

Fig. 8. FTIR spectrum of $SnSeO_3/ZnSeO_3$ nanocomposite.

3.5. Low temperature magnetic studies

Figure 9 and Figure 10 shows $SnSeO_3/ZnSeO_3$ nanocomposite confirming diamagnetic nature of sample[21] at 300K and 5K. But, the expanded M-H curve shown in Figure 11 exhibits interesting super paramagnetic nature between -0.15Tesla to 0.15Tesla.

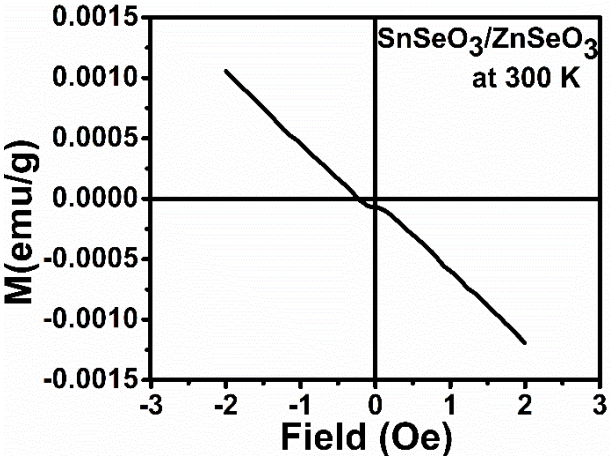

Fig. 9. M-H curve of $SnSeO_3/ZnSeO_3$ nanocomposite at 300K.

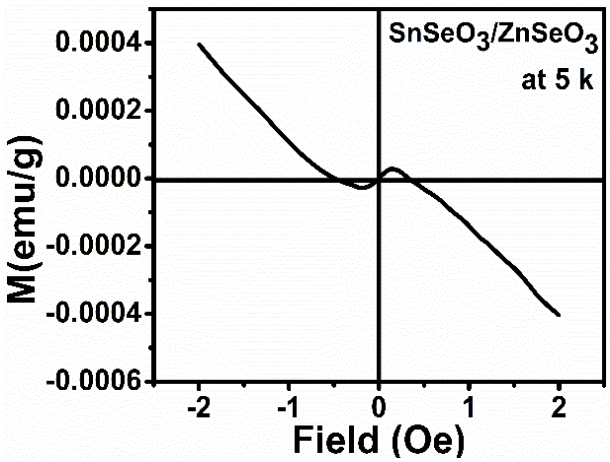

Fig. 10. M-H curve of $SnSeO_3/ZnSeO_3$ nanocomposite at 5K.

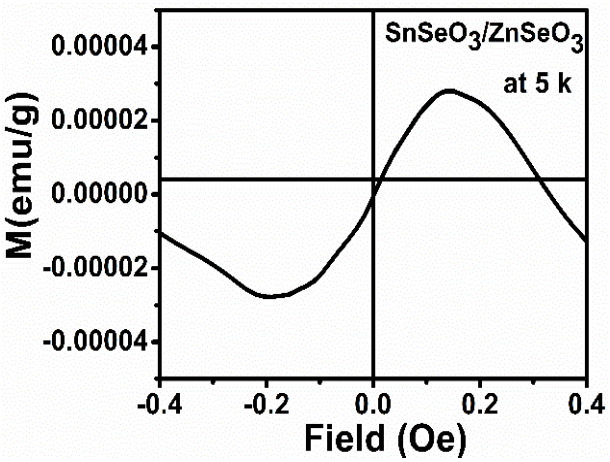

Fig. 11. Expanded M-H curve of $SnSeO_3/ZnSeO_3$ nanocomposite at 5K.

4. Conclusions

Nanocomposite $SnSeO_3/ZnSeO_3$ which belongs to oxychalcogenides has been synthesized by hydrothermal method. EDAX of $SnSeO_3/ZnSeO_3$ nano composites shows that the sample is composed of Sn, Zn, Se and O elements, which confirm the product purity and confirms the perfect formation of $SnSeO_3/ZnSeO_3$ nano composite. It shows an interesting morphology of rectangular bar. Particle size is determined as 137.3nm. XRD confirmed the perfect formation of $SnSeO_3/ZnSeO_3$. It is a strong candidate for optoelectronic applications. It exhibits 5.52 eV energy gap. The calculated Urbach energy is 0.0635 eV. The optical energy gap yielded a refractive index of 1.926. Strong efficient emission is obtained in the UV (~387.7 nm) area, weak emission in the green (~520.7 nm) region, and moderate emission in the red (~788.7 nm) part of the PL emission spectrum.

The peak in the UV region at 387.7nm may be due to radiative electron-hole recombination and it makes the candidate a promising material for display applications. The emission peaks in the visible range may be attributed to different surface imperfections of Schottky and Frenkel kinds, oxygen vacancies and Sn –interstitials or Zn -interstitials. Nanoparticles have the potential to be employed as optoelectronic devices, luminescence detectors, and ultraviolet photo-conductive detectors. The bands observed in FTIR are well assigned and confirms Se-O bond, Zn-O bond and Sn-O bonds in finger print region. The sample exhibits diamagnetic nature at 300K and 5K. It also exhibits interesting super paramagnetic nature at 5K between -0.15Tesla to 0.15Tesla.

Acknowledgments

Authors are thankful to University Science Instrumentation Centre, Alagappa University, Karaikudi, Tamilnadu, India for access to their low temperature facilities.

References

[1] M. V. Kulkarni, A. K. Viswanath, P. K. Khanna, Int. J. Polym. Mater. and Polym. Biomater. **55**, 501(2006); https://doi.org/10.1080/00914030500210358
[2] J. C. Lacroix, K. K. Kanazawa, A. Diaz, J. Electrochem. Soc. 136, 1308(1989); https://doi.org/10.1149/1.2096912

[3] Y. F. Shi, W. B. Wei, X. T. Wu, H. Lin, Q. L. Zhu, Dalton Trans. **50**, 4112(2021); https://doi.org/10.1039/D1DT00222H
[4] F. Wang, S. Yang, J. Wu, X. Hu, Y. Li, H. Li, X. Liu, J. Luo, T. Zhai, InfoMat **3**, 1251(2021); https://doi.org/10.1002/inf2.12215
[5] H. Hiramatsu, H. Yanagi, T. Kamiya, K. Ueda, M. Hirano, H. Hosono, Chem. of Mater. **20**,326 (2008); http://dx.doi.org/10.1021/cm702303r
[6] N. Zhang, J. Sun, H. Gong, Coatings **9**, 137(2019); https://doi.org/10.3390/coatings9020137
[7] S. Tippireddy, P. K. Das, S. Das, R. C. Mallik, ACS Appl. Energy Mater. **4**, 2022(2021); https://doi.org/10.1021/acsaem.0c02770
[8] S. J. Clarke, P. Adamson, S. J. Herkelrath, O. J. Rutt, D. R. Parker, M. J. Pitcher, C. F. Smura, Inorg. Chem. **47**, 8473(2008); https://doi.org/10.1021/ic8009964
[9] M. Wu, X. C. Zeng, Nano Lett. **17**,6309(2017); https://doi.org/10.1021/acs.nanolett.7b03020
[10] H. Kabbour, E. Janod, B. Corraze, M. Danot, C. Lee, M. Whangbo, L. Cario, J. Am. Chem. Soc **130**, 8261(2008); https://doi.org/10.1021/ja711139g
[11] https://oqmd.org/materials/entry/1758603
[12] https://next-gen.materialsproject.org/materials/mp-4682?chemsys=Zn-Se-O
[13] A. Modwi, K. K. Taha, L. Khezami, Zeitschrift für PhysikalischeChemie **235**, 745 (2021); https://doi.org/10.1515/zpch-2019-1473
[14] https://en.wikipedia.org/wiki/Ultraviolet%E2%80%93visible_spectroscopy
[15] Unit-I Ultra-violet and Visible Spectroscopy; https://bbec.ac.in/wp-content/uploads/2015/08/Spectroscopy_UV-Visible.pdf
[16]4.4:UV-Visible Spectroscopy - Chemistry LibreTexts. https://chem.libretexts.org/Bookshelves/Analytical_Chemistry/Physical_Methods_in_Chemistry_and_Nano_Science_%28Barron%29/04%3A_Chemical_Speciation/4.04%3A_UVVisible_Spectroscopy
[17] M. Tahenti, N Issaoui, T. Roisnel, S. Aleksandr, Kazachenko, A. Maximiliano, Iramain, Silvia Antonia Brandan, Omar Al-Dossary, A.S. Kazachenko, Houda Marouan, Zeitschrift für Physikalische Chemie **237**, 1775 (2023); https://doi.org/10.1515/zpch-2023-0332
[18] Y. Slimani, S. S. Meena, S. E. Shirsath, E. Hannachi, M. A. Almessiere, A. Baykal, R. Sivakumar, M. Khlid, Batoo, A. Thakur, I. Ercan, B. Özçelik, Zeitschrift für Physikalische Chemie **237**, 1753(2023); https://doi.org/10.1515/zpch-2023-0215
[19] M. K. Halimah, M. F. Faznny, M. N. Azlan, H. A. A. Sidek, Results Phys. **7**, 581(2017); https://doi.org/10.1016/j.rinp.2017.01.014
[20] H. Saudi, G. Adel, Optics **6**, 17(2018)
[21] Gang Xiong, K. B. Ucer, R. T. Williams, U. Pal, J. Garcia Serrano, Phys. Stat. Solidi C **3**, 3577(2006); https://doi.org/10.1002/pssc.200672164
[22] B. Rudraswamy, N. Dhananjaya, IOP Conf Series: Mater. Sci. Eng. **40**, 012034 (2012); https://doi.org/10.1088/1757-899X/40/1/012034
[23] A. T. M. Anishur Rahman, K. Vasilev, P. Majewski, J. Colloid Interface Sci. **354**, 592(2011); https://doi.org/10.1016/j.jcis.2010.11.012
[24] R. K. Tamrakar, D. P. Bisen, K. Upadhyay, M. Sahu, I. P. Sahu, N. Bramhe, Superlattices Microstruct. **88**, 382(2015); https://doi.org/10.1016/j.spmi.2015.09.033
[25] A. Dehelean, S. Rada, A. Popa, E. Culea, J. Mol. Struct. **1036**, 203(2013); https://doi.org/10.1016/j.molstruc.2012.11.051
[26] M. Mazhdi, M. J. Tafreshi, Appl. Phys. A **124**, 863(2018); https://doi.org/10.1007/s00339-018-2291-0
[27] M. W. Maswanganye, G. L. Kabongo, L. E. Mathevula, B. M. Mothudi, M. S. Dhlamini, Sci. Rep. **13**, 20131(2023); https://doi.org/10.1038/s41598-023-47436-7
[28] Mehar Bhatnagar, Vishakha Kaushik, Akshey Kaushal, Mandeep Singh, Bodh Raj Mehta, AIP Adv. **6**, 095321(2016); http://dx.doi.org/10.1063/1.4964313
[29] Mohan Jag, Organic Spectroscopy, Narosa Publication House, New Delhi, 2000
[30] R.M. Silverstein, F.X. Webster, Spectrometric identification of organic compounds, John Wiley and Sons Inc, USA, 1991
[31] K. Nakamoto, Infrared and Raman spectra of inorganic and coordination compounds, John Wiley & Sons, USA, 1986

[32] Yu-Wei Chena, Lu Lia, Alessandro D'Ulivo b, Nelson Belzile, Anal. Chim. Acta **577**, 126(2006); https://doi.org/10.1016/j.aca.2006.06.020
[33] Rajendran Sorna Prema, Sengodan Kandasamy, J. Nanosci. **2017**, 1(2017); https://doi.org/10.1155/2017/8348507
[34] Sunday Wilson Balogun, Olusola Oladele James, Yekini Kolawole Sanusi, Oyeshola Hakeem Olayinka, SN Appl. Sci. **2**, 504(2020); https://doi.org/10.1007/s42452-020-2127-3
[35] Santos T. Chartier , C. Pagnoux, J. F. Baumard, C. V. Santillii, S. H. Pulcinelli, A. Larbot, J. Eur. Ceram. Soc. **24**, 3713(2004); https://doi.org/10.1016/j.jeurceramsoc.2004.03.003